Partially Coherent Quantitative Phase Retrieval for EUV Lithography

Rene A. Claus[1,*], Yow-Gwo Wang[1], Markus P. Benk[2], Kenneth A. Goldberg[2], Patrick P. Naulleau[2], Andrew R. Neureuther[1] and Laura Waller[1]

[1] *University of California, Berkeley, CA, 94709, USA*
[2] *CXRO, Lawrence Berkeley National Lab, Berkeley, CA, 94709, USA*
[*] *reneclaus@gmail.com*

Abstract: We present a phase recovery algorithm based on the Weak Object Transfer Function. The algorithm is iteratively extended to also apply to non-weak objects. We demonstrate the algorithm on an EUV multilayer defect imaged through-focus on SHARP with both a standard zone plate and a phase contrast zone plate.

OCIS codes: (110.1758) Computational imaging; (100.5070) Phase retrieval; (110.3010) Image reconstruction techniques

Extreme Ultraviolet (EUV) lithography mask inspection presents a unique need for accurate quantitative phase imaging techniques. One of the key challenges of EUV lithography is the availability of defect-free photomasks [1]. EUV photomasks are multilayer mirrors on a glass substrate that are subsequently patterned with an absorber. These photomasks are used to print semiconductor devices. EUV technology operates at a wavelength of 13.5*nm* with features as small as 12 nm after magnification.

One of the major problems affecting EUV masks is phase defects that change the pattern being printed. These defects form when the multilayer conformally covers particles or pits in the substrate or particles that are added during the multilayer deposition process. Several approaches to mitigating the impact of these defects are being considered. Pattern Shift is the process of shifting the absorber pattern so that it covers all the defects on the mask in such a way that they will not affect printing [2]. Another approach is to locally etch the multilayer to compensate the phase of the defects [3]. It is also possible to modify the absorber pattern so that it will still print working devices even with a defect nearby [4]. Each of these methods benefit from quantitative information about the amplitude and phase of the defect by allowing the effectiveness of possible repairs to be evaluated computationally.

We have developed an algorithm based on the Weak Object Transfer Function (WOTF) that is well suited to the needs of EUV mask inspection and repair [5]. The algorithm is able to consider partial coherence, arbitrary pupil functions, and can combine any number of measurements (≥ 2) to recover the phase and amplitude of the object. The use of partially coherent illumination permits greater light throughput and allows higher resolution measurements of the defect than coherent light. The ability to use different numbers of images allows trade-off between resilience to noise and throughput. We extend the accuracy of the algorithm to objects that are not strictly weak using an approach that iteratively strengthens the weak object approximation.

We experimentally verified our algorithm using data from the SEMATECH High Numerical Aperture Actinic Reticle Review Project (SHARP) microscope at Lawrence Berkeley National Laboratory [6]. SHARP is a zone plate microscope, which allowed us to replace the standard zone plate with a phase contrast zone plate to produce two distinct measurements of the same defect [7]. Applying the algorithm to each set of images independently allowed us to confirm that the algorithm recovered the correct phase and amplitude.

1. Algorithm

Under the Weak Object Assumption (WOA) it is possible to express the intensity as a linear function of the electric field using the WOTF [8]. This transfer function can be inverted to recover the field [9]. The WOA requires that the sample is weakly scattering so that the intensity variations depend primarily on the interference between the unscattered light and scattered light—the interference between scattered light and itself is assumed to be negligible. The measured intensity can then be described by the sum of two convolutions:

$$I = I_0 + E_{re} * K_{re} + E_{im} * K_{im} + I_e \tag{1}$$

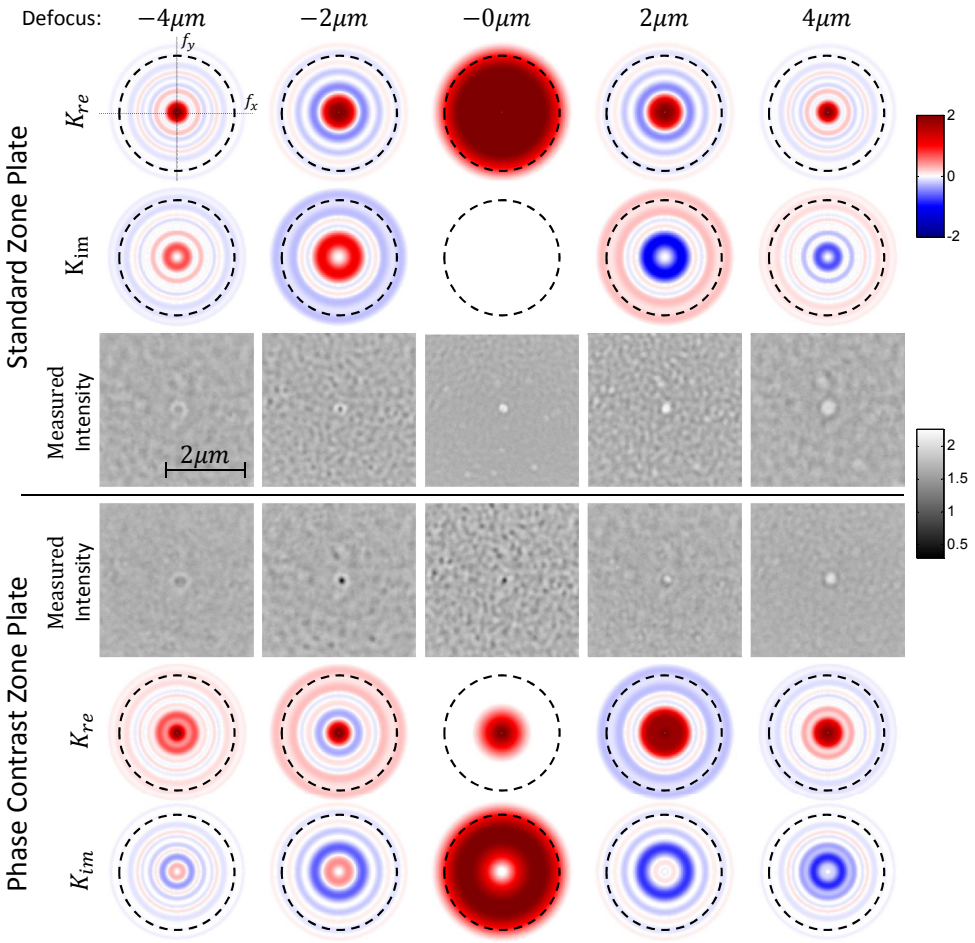

Fig. 1. A subset of the measurements taken using the standard zone plate (top) and phase contrast zone plate (bottom) of an EUV photomask defect are shown. The focus position for each image is shown at the top. The real and imaginary transfer functions for each image are also shown. They are shown in Fourier space with the NA marked by the dashed circle.

where I is the intensity, E_{re} is the real part of the object without the DC, E_{im} is the imaginary part of the object, I_e is the error in the approximation. The WOTF for the real and imaginary parts of the object, $\widetilde{K_{re}}$ and $\widetilde{K_{im}}$, are given by

$$\widetilde{K_{re}} = (\widetilde{P}\cdot\widetilde{J})\star\widetilde{P} + \widetilde{P}\star(\widetilde{P}\cdot\widetilde{J}) \qquad \text{and} \qquad \widetilde{K_{im}} = (\widetilde{P}\cdot\widetilde{J})\star\widetilde{P} - \widetilde{P}\star(\widetilde{P}\cdot\widetilde{J}) \tag{2}$$

where a $\widetilde{tilde}$ represents the Fourier transform, $\widetilde{P}$ is the pupil function, and $\widetilde{J}$ is the source intensity distribution.

By ignoring I_e, Eq. (1) can be solved using multiple measurements by representing it in frequency space as a multiplication and writing the sum of products as a matrix equation for each frequency:

$$\begin{bmatrix} \widetilde{I_1}(f_i) \\ \vdots \\ \widetilde{I_n}(f_i) \end{bmatrix} = \begin{bmatrix} \widetilde{K_{re}^1}(f_i) & \widetilde{K_{im}^1}(f_i) \\ \vdots & \vdots \\ \widetilde{K_{re}^n}(f_i) & \widetilde{K_{im}^n}(f_i) \end{bmatrix} \begin{bmatrix} \widetilde{E_{re}}(f_i) \\ \widetilde{E_{im}}(f_i) \end{bmatrix} \tag{3}$$

Each row in this matrix represents a measurement and the equation can be solved using least squares, combining the information from multiple images into a single estimate of the object. As long as the transfer functions vary among the measured images, the equation will have a solution. Measuring the object through-focus will produce such a measurement by varying P. These measurements can be taken under partially coherent illumination because the transfer functions consider the source shape, $\widetilde{L}$. The use of least squares has the added benefit of adding resilience to noise when using more measurements.

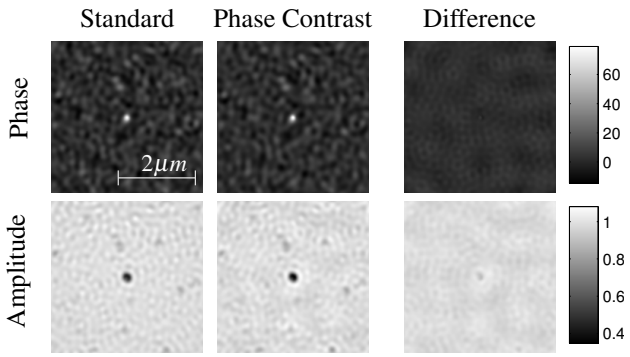

Fig. 2. The recovered phase in degrees (top) and amplitude (bottom) are shown for the standard zone plate and phase contrast zone plate measurements. The defect had a peak phase of 130 degrees and a minimum amplitude of 0.3. The maximum difference between the two recovered fields is 0.09 for amplitude and 8 degrees for phase.

The WOA requires that $|E_{re} + \mathrm{i}E_{im}| \ll 1$. This restriction is relaxed by subtracting the error term in the approximation, I_e, from the measurements. This can be done iteratively by computing an estimate of the object, E_{re} and E_{im}, and then using that to calculate an estimate of I_e. After each iteration, the estimate of the object will improve along with the estimate of the error in the approximation.

2. Experiment

To verify the algorithm we measured a native EUV multilayer defect using both a standard zone plate and a phase contrast zone plate on SHARP. The phase contrast zone plate had a 90 degree phase shift region of radius $0.3 \cdot NA$. For each lens, 21 through-focus images in the range ± 5 μm were captured. For both measurements, the NA was 0.0825, the wavelength was 13.5 nm, and the illumination was a $0.25 \cdot NA$ disk. Traditionally phase contrast is a non-quantitative method, but with our algorithm and through-focus data we can recover quantitative phase from phase contrast images.

Representative images from both measurements are shown in Fig. 1 along with the corresponding transfer functions. The measurements using the two lenses are qualitatively very different—the defect appears dark in one case and bright in the other and the surrounding roughness produces high contrast speckle at focus only in the phase contrast measurements. This behavior is explained by the transfer functions where K_{re} and K_{im} are approximately switched between the standard zone plate measurements and phase contrast zone plate measurements. The algorithm was applied independently to each focus series and the recovered phase and amplitude, as well as the difference in the two results, are shown in Fig. 2. The defect has a peak phase of 130 degrees and a minimum amplitude of 0.7. The maximum error between the two recovered fields is 0.09 for amplitude and 8 degrees. Since the measurements are qualitatively very different but produce the same phase and amplitude, it is highly likely that the algorithm has recovered the correct field of the object. Moreover, it is able to do this under partially coherent illumination, for a complicated pupil, on an object that does not satisfy the weak object approximation.

References

1. F. Goodwin *et al.*, "Recent advances in SEMATECH's mask blank development program, the remaining technical challenges, and future outlook," Proc. SPIE **8886**, 88,860C–88,860C–9.
2. P.-Y. Yan *et al.*, "EUVL multilayer mask blank defect mitigation for defect-free EUVL mask fabrication," Proc. SPIE **8322**, 83,220Z–83,220Z–10 (2012).
3. R. Jonckheere *et al.*, "Repair of natural EUV reticle defects," Proc. SPIE **8166**, 81,661G–81,661G–11 (2011).
4. T. Bret *et al.*, "Closing the gap for EUV mask repair," Proc. SPIE **8322**, 83,220C–83,220C–9 (2012).
5. R. A. Claus *et al.*, "Phase Measurements of EUV Mask Defects," Proc. SPIE (2015).
6. K. A. Goldberg *et al.*, "Commissioning an EUV mask microscope for lithography generations reaching 8 nm," Proc. SPIE **8679**, 867,919–867,919–10 (2013).
7. Y.-G. Wang *et al.*, "Enhancing defect detection with Zernike phase contrsat in EUV multilayer blank inspection," Proc. SPIE **9422**, 942,247 (2015).
8. C. J. R. Sheppard, "Defocused transfer function for a partially coherent microscope and application to phase retrieval," J. Opt. Soc. Am. **21**, 828–831 (2004).
9. S. S. Kou *et al.*, "Quantitative phase restoration by direct inversion using the optical transfer function." Opt. Lett. **36**, 2671–3 (2011).